

Diffusion Studies of Dihydroxybenzene Isomers in Water–Alcohol Systems

Dale J. Codling,[†] Gang Zheng,[†] Tim Stait-Gardner,[†] Shu Yang,[‡] Mathias Nilsson,^{§,||} and William S. Price^{*,†}

[†]Nanoscale Organisation and Dynamics Group, School of Science and Health, University of Western Sydney, Penrith, NSW 2751, Australia

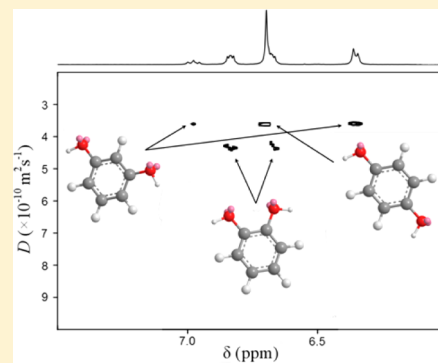
[‡]CAS Key Lab for Biological Effects of Nanomaterials and Nanosafety, National Center for Nanoscience and Technology, No.11 BeiYiTiao ZhongGuanCun, 100190 Beijing, People's Republic of China

[§]Department of Food Science, Faculty of Science, University of Copenhagen, Rolighedsvej 30, DK - 1958 Frederiksberg C, Denmark

^{||}School of Chemistry, University of Manchester, Oxford Road, Manchester M13 9PL, United Kingdom

S Supporting Information

ABSTRACT: Nuclear magnetic resonance diffusion studies can be used to identify different compounds in a mixture. However, because the diffusion coefficient is primarily dependent on the effective hydrodynamic radius, it is particularly difficult to resolve compounds with similar size and structure, such as isomers, on the basis of diffusion. Differential solution interactions between species in certain solutions can afford possibilities for separation. In the present study, the self-diffusion of the three isomers of dihydroxybenzene (i.e., (1,2-) catechol, (1,3-) resorcinol, and (1,4-) hydroquinone) was studied in water, aqueous monohydric alcohols (i.e., ethanol, 1-propanol, *tert*-butanol), and aqueous ethylene glycol. These systems allowed the effects of isomerism and differential solvent interactions on diffusion to be examined. It was found that, while in aqueous solution these isomers had the same diffusion coefficient, in water–monohydric alcohol systems the diffusion coefficient of catechol differed from those of resorcinol and hydroquinone. The separation was found to increase at higher concentrations of monohydric alcohols. The underlying chemical reasons for these differences were investigated.



INTRODUCTION

Nuclear magnetic resonance (NMR) is an important tool for the characterization of molecules. Using ordinary NMR techniques, however, it is generally very difficult to separate the resonances of different species in a mixture. Pulsed gradient spin–echo (PGSE) NMR diffusion measurements allow the resonances of the different species in a mixture to be separated on the basis of the translational (or self-) diffusion coefficients of the different species.^{1–5} PGSE data can be displayed in 2-D format with diffusion as the second dimension to visualize the data as diffusion-ordered spectroscopy (DOSY).^{6,7} The two most important factors affecting the ability of PGSE NMR to resolve component spectra are spectral resolution and the relative difference in diffusion coefficients. When spectral resolution allows and each component is monodisperse, resonances with diffusion coefficients differing by as little as 1% can be resolved.⁸ In the general case, when resonances overlap and/or components are polydisperse, it is much more difficult; a number of processing methods have been developed with the view of extracting the most information from such data.^{9,10} The diffusion coefficient of a species depends on both its (hydrodynamic) size and its intermolecular interactions to a matrix. For example, the binding of a species to a larger

molecule or network of molecules will alter the effective hydrodynamic radius of the species. Aqueous systems with their complicated hydrogen-bonding behavior are prime examples of associative networks affecting diffusive behavior.^{11–13} Consequently, resonances of isomeric species, which would otherwise have similar diffusion coefficients, might be separated on the basis of diffusion if they have different binding properties to the matrix. Thus, modulation of the matrix can be used to effect diffusion resolution as in a matrix-assisted DOSY (MAD) experiment.² Indeed, micelles have been shown to separate the diffusion of monomethoxyphenol isomers,^{2,14–16} and mixtures of epimers of the flavanone glycoside naringin were resolved using diffusion with the addition of β -cyclodextrin.¹⁷ The addition of lanthanide shift reagents to enhance chemical shift resolution for a mixture of species had the additional effect of enhancing diffusion resolution of the species.¹⁸

While there is an immediate usefulness to mixture analysis by separating different species, it is also of interest to understand

Received: November 8, 2012

Revised: February 4, 2013

Published: February 6, 2013

the underlying chemical basis of why some isomeric species with comparable hydrodynamic radii in simple solution are separable based on diffusion. The three isomers of dihydroxybenzene (i.e., resorcinol (R), catechol (C), and hydroquinone (H); Figure 1) form an interesting system. The separation of

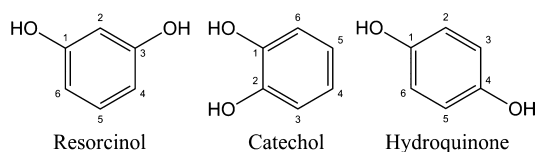


Figure 1. The molecular structures of the dihydroxybenzene isomers, resorcinol (R), catechol (C), and hydroquinone (H). The atom numbering for each isomer is shown.

these isomers is of particular interest to column chromatography,^{19–22} with hydrophobic and hydrophilic interactions allowing extraction of these isomers. In aqueous solution, these isomers have similar diffusion coefficients. It has been shown that the isomers R, C, and H can be resolved using PGSE NMR diffusion measurements by the introduction of micelles,² where both normal and reverse micelles separated the diffusion of the isomers. It was proposed that the R, C, and H solutes have a different degree of incorporation into the micellar core due to the difference in their hydrophobicity.

In the present study, the possibility of separating the isomers R, C, and H on the basis of their respective self-diffusion coefficients when dissolved in different alcohol-containing solvents was investigated using PGSE NMR diffusion measurements. Although measurements at low solute concentrations could be described as tracer diffusion, hereinafter and consistent with the NMR literature all measurements are termed self-diffusion. Water–alcohol solutions, in this case ethanol (EtOH), 1-propanol (1-PrOH), and *tert*-butanol (*t*-BuOH), provide suitable systems to investigate if the differences in the diffusion of the isomer are related to solution structuring. Such structuring is of wide ranging significance with, for example, water–alcohol solvents shown to affect protein structure.²³ The structuring of water and monohydric alcohol varies across the concentration range of alcohol.^{24,25} It has been shown using PGSE NMR diffusion measurements that at low alcohol mole fraction (x_A) a hydration network of water molecules forms around the alcohol molecules; in the range $x_A = 0.2$ – 0.3 , the organization of these clathrate-like structures is at its greatest.²⁴ As the concentration of alcohol is increased, the self-association of alcohol complicates this process, and at higher x_A the water and alcohol become increasingly independent of one another. ¹H NMR diffusion, spin–lattice (T_1), and spin–spin (T_2) relaxation studies of methanol–water systems have shown that hydrogen-bonding interactions between water and methanol were temperature dependent.^{26,27} The influence of these interactions increased with temperature with a maximum T_1 and T_2 at 245 K, and above this temperature there was greater interaction between the methanol and water molecules. There have been numerous other studies into the structuring of alcohol–water systems including EtOH–water^{28–32} and *t*-BuOH–water systems.³¹ Ethylene glycol has been included in this study to offer some comparison to the solution dynamics of monohydric alcohols. Because of its two hydroxyl groups, ethylene glycol can be related more to water than monohydric alcohol, with both being able to form up to four hydrogen bonds per molecule.³³

Ethylene glycol is also more likely to form three-dimensional hydrogen-bonded structures similar to water,³⁴ with a preferred gauche conformation in solution,^{35,36} as opposed to monohydric alcohols that form linear chains.

A recent study using density and speed of sound measurements showed a difference in the interactions between R, C, and H isomers with water.³⁷ The different positions of the hydroxyl groups resulted in the molecules interacting differently with solvents. It was shown that isomer C had the strongest hydrophilic interactions among the three isomers due to its greater dipole moment. The formation of clathrate-like structures was expected for all three isomers with isomer C seeing less of this formation as the *ortho*-position of the OH groups shielded the hydrophobic surface, which did not occur when the OH groups were further apart such as in the *meta*- and *para*-positions. It was proposed that the isomers R and C formed solute–solvent complexes.^{38,39} It was shown, using *ab initio* and density functional methods, that isomer C had a preference for forming a solute–solvent association with three molecules of water and isomer R had a preference for forming an association with two molecules of water. OH groups played important roles in both cases. The formation of the dimers of the R, C, and H isomers was modeled using density function theory and MP2 calculations.⁴⁰ This comparative study of the energy of interaction showed that the preferred orientation for each molecule in a dimer was with the aromatic rings being perpendicular to each other.

When investigating the properties of liquids, the effects of hydrogen bonds are especially pertinent in aqueous solutions. The formation of a hydrogen bond changes the charge distribution of a water molecule in such a way that it is capable of forming another stronger hydrogen bond.⁴¹ This is an important characteristic of water, which results in a preferential orientation of hydration shells around nonpolar solutes.^{42,43} Monohydric alcohols can form up to two hydrogen bonds, one acceptor and one donor. Water–alcohol is a complex system to study due to its solution structuring giving a nonlinear relationship to the proportions of its components, and it is important to consider not only the hydrogen bonds occurring between the water and alcohol molecules but also the possibility of alcohol–alcohol bonds in preference to alcohol–water bonds. In this study, heavy water (D_2O) was used instead of light water (H_2O) to avoid the problems associated with the strong ¹H NMR signal from H_2O . The structure of D_2O is similar to H_2O , although D_2O is a more structured liquid than H_2O , forming more hydrogen bonds; the molecular arrangement of D_2O molecules is geometrically more tetrahedral than H_2O .⁴⁴ D_2O also has a higher viscosity than H_2O ,⁴⁵ and thus a lower diffusion coefficient (i.e., 1.87 versus $2.30 \times 10^{-9} \text{ m}^2 \text{ s}^{-1}$ at 298 K).^{11,13,46} As the deuterium will exchange with hydrogen from H_2O and hydroxyl groups, at higher concentrations of alcohol in D_2O –alcohol systems there will be a greater amount of H_2O .

The diffusion of a species is directly related to the molecular size of the species and the nature of the solvent. This is modeled using the Stokes–Einstein–Sutherland equation,^{47–49} which in the stick boundary condition has the form:

$$D = \frac{kT}{6\pi\eta r_s} \quad (1)$$

where k is the Boltzmann constant, η is the solvent viscosity, T is the temperature, and r_s is the effective hydrodynamic (or

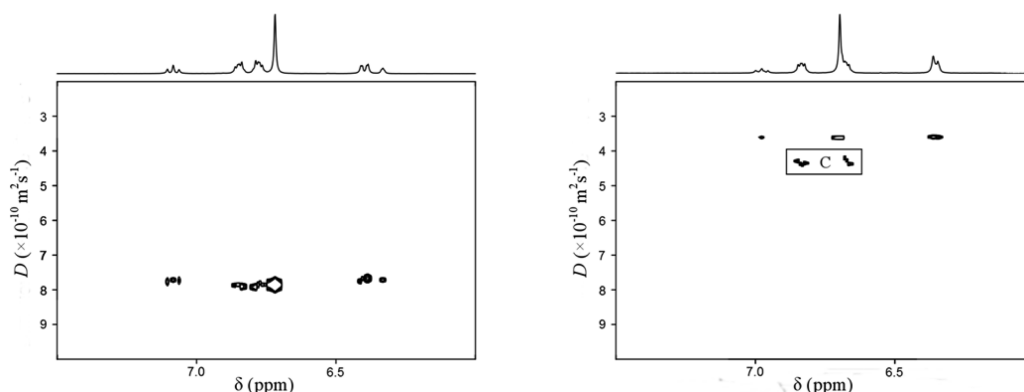


Figure 2. DOSY spectra of a mixture of R, C, and H in D_2O (left) and D_2O –ethanol with $x_{EtOH} = 0.8$ (right) at 298 K. The change of solvent alters the diffusion behavior of the solutes so that C is well resolved in the diffusion dimension when EtOH is present.

Stokes) radius. Strictly, eq 1 only holds at infinite dilution and when the solute sees the solvent as continuum (i.e., when the solute molecules are large as compared to the solvent molecules). Although modifications to eq 1 have been derived for nonspherical solutes,⁵⁰ its present form is sufficient for the semiquantitative analysis of the diffusion data presented here.

In the present work, it was found that while the isomers R, C, and H had similar diffusion coefficients in aqueous solution, the addition of a monohydric alcohol to the system caused the diffusion coefficient of isomer C to separate from those of isomers R and H. To clarify the underlying solution dynamics, the diffusion of these species was investigated in solutions with various concentrations of ethanol, 1-propanol, *tert*-butanol, and ethylene glycol. The diffusion data were used to determine the Stokes radii and allow comparison between the isomers. The results are then discussed in relation to previous water–alcohol studies.

EXPERIMENTAL METHODS

Materials and NMR Samples. Resorcinol (99%), catechol ($\geq 99\%$), hydroquinone ($\geq 99\%$), ethanol (96%), 1-propanol (99%), and *tert*-butanol (99%) were purchased from Sigma-Aldrich, D_2O (99.9%) was purchased from Cambridge Isotope Laboratories, and ethylene glycol ($>99\%$) was obtained from Chem-Supply. All chemicals were used without further purification. A stock solution ~ 350 mM of each of the isomers R, C, and H was prepared in D_2O for the preparation of samples of various mole fractions.

Aliquots (500 μL) were dispensed into 5 mm NMR tubes (Wilmad 528-PP-7). Unless stated otherwise, the concentration of each isomer in the NMR samples was ~ 15 mM. For experiments with high x_A , the sample was placed into 61 μL straight capillary tubes (Wilmad 529-D), which were coaxially inserted into 5 mm NMR tubes (Wilmad 528-PP-7) containing D_2O .

NMR Experiments. Unless stated otherwise, all 1H NMR measurements were performed on a 400 MHz Bruker Avance spectrometer at 298 K, using a 5 mm BBO probe equipped with a z gradient coil producing a maximum gradient strength of 0.53 T m^{-1} . All samples had reached equilibrium prior to measurement. An initial diffusion experiment (Figure 2) was acquired with the Oneshot^{51,52} sequence with a diffusion encoding pulse duration, δ , of 3 ms, a diffusion delay, Δ , of 0.1 s, and 15 nominal gradient amplitudes, g , ranging from 0.034 to 0.27 T m^{-1} chosen to give equal steps in gradient squared. The data were corrected for instrumental inconsistencies by

reference deconvolution and the figure produced in the DOSY Toolbox.^{10,53} However, all subsequent data were acquired using a stimulated spin–echo pulse sequence containing bipolar diffusion weighting gradients postfixed with a WATERGATE⁵⁴ sequence with a soft π pulse selectively inverting the R, C, and H isomer resonances (see Supporting Information). Typical acquisition parameters were $\delta = 2$ ms, $\Delta = 0.1$ s, and g increasing from 0.01 to 0.50 T m^{-1} linearly in 16 steps with a sufficient recycle delay to allow full relaxation. 1H chemical shifts were measured from a spectrum acquired using a standard pulse and collect experiment.

Data Analysis. The NMR diffusion data were analyzed by nonlinear least-squares regression of the appropriate attenuation expression using OriginPro 8.1 (OriginLab).⁴ The error estimates given in the figures below are those from the data fitting. The Stokes radii of the isomers were calculated using the Stokes–Einstein–Sutherland equation (eq 1) with the measured D values of the R, C, and H isomers and literature values for viscosities^{55–59} of the solvent systems interpolated using a fifth-order polynomial in OriginPro 8.1.

RESULTS

The results of a preliminary diffusion study presented in DOSY format are given in Figure 2. The results clearly show the resolution of the C resonance on the basis of diffusion in the presence of ethanol at $x_{EtOH} = 0.8$.

The diffusion of the R, C, and H isomers was investigated to see the effect of alcohol concentration on diffusion. The results at various x_A of EtOH, 1-PrOH, *t*-BuOH, and ethylene glycol in D_2O are presented in detail.

Ethanol. The diffusion of R, C, and H in mixtures with increasing x_{EtOH} is shown in Figure 3. The diffusion of the isomers initially decreased before gradually increasing as x_{EtOH} increased. The diffusion of each of the isomers followed a trend similar to that of the EtOH across the entire x_{EtOH} range. The diffusion of EtOH in this system followed the same trend as in the H_2O –EtOH system given in Price et al.²⁴ This suggested that the D_2O and EtOH interact in a similar fashion in both systems. The diffusion minima for all three isomers lie in the range $x_{EtOH} = 0.2$ – 0.3 . This region saw the greatest aggregation of EtOH and H_2O .²⁴ From $x_{EtOH} \sim 0.2$ on, there was a distinct separation of isomer C from the isomers R and H in diffusion. The diffusion of isomer C differs from isomers R and H by over 18% at $x_{EtOH} \sim 0.9$. In this region, the H_2O loses its hydrogen-bond network and exists as single molecules in the EtOH solution.²⁴

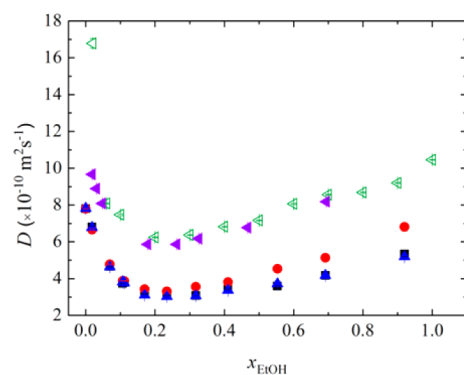


Figure 3. Diffusion coefficients (D) of R (■), C (red ●), and H (blue ▲) at ~ 15 mM and EtOH (purple left-facing ▲) in samples at various ethanol mole fractions (x_{EtOH}) in D_2O measured at 298 K. The data for EtOH (green left-facing ▲) in the H_2O –alcohol system taken from ref 24 are shown for comparison. The error bars are generally smaller than the symbols.

To exclude self-aggregation as a possible cause for the separation occurring between the R, C, and H molecules, diffusion measurements of the isomers were conducted over a range of concentrations at $x_{\text{EtOH}} = 0.22$. This x_{EtOH} was chosen as separation had started to occur, and it saw the greatest structural association between water and EtOH.^{24,28} The results suggested that no aggregation between the isomers occurred in this system as the diffusion of each isomer was only slightly affected by concentration changes (Figure 4).

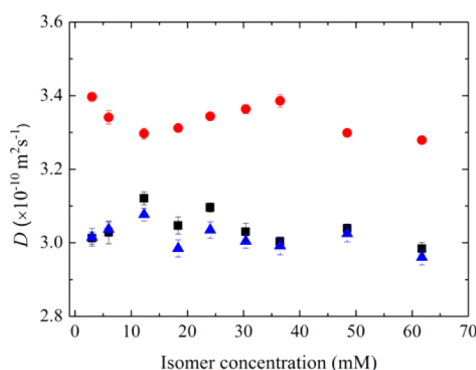


Figure 4. Diffusion of R (■), C (red ●), and H (blue ▲) at different concentrations at $x_{\text{EtOH}} = \sim 0.22$ in D_2O measured at 298 K.

1-Propanol. The diffusion of R, C, and H mixtures versus 1-PrOH mole fraction is shown in Figure 5. Initially, the diffusion of the isomers decreased rapidly as $x_{1\text{-PrOH}}$ increased, the C diffusion then gradually increased, whereas the isomers R and H plateau before increasing when $x_{1\text{-PrOH}} > 0.5$. From $x_{1\text{-PrOH}} = 0.05$ on, there is a distinct separation of the diffusion for isomer C from the diffusion for isomers R and H, with the separation gradually increasing at higher $x_{1\text{-PrOH}}$. The diffusion of isomer C is 25% greater when $x_{1\text{-PrOH}} \geq 0.62$. The 1-PrOH diffusion followed a trend similar to what is given in the literature for H_2O –1-PrOH.^{60,61}

tert-Butanol. The diffusion of R, C, and H in mixtures with increasing $x_{t\text{-BuOH}}$ is shown in Figure 6. As $x_{t\text{-BuOH}}$ increased, the diffusion of the isomers decreased initially before leveling out for R and H and increasing slightly for C when $x_{t\text{-BuOH}} > 0.2$. The diffusion coefficient for each of the isomers followed a trend similar to that of $t\text{-BuOH}$ across the entire $x_{t\text{-BuOH}}$ range.

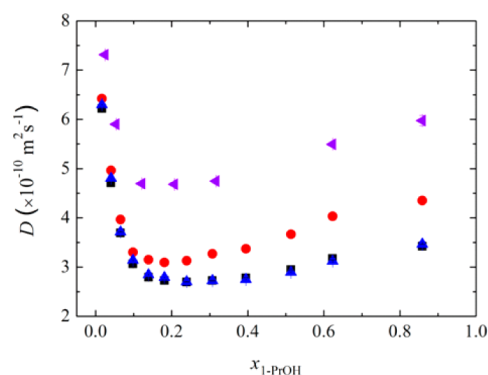


Figure 5. Diffusion coefficients (D) of R (■), C (red ●), and H (blue ▲) at ~ 15 mM and 1-PrOH (purple left-facing ▲) in samples at various 1-propanol mole fractions ($x_{1\text{-PrOH}}$) in D_2O measured at 298 K. The error bars are generally smaller than the symbols.

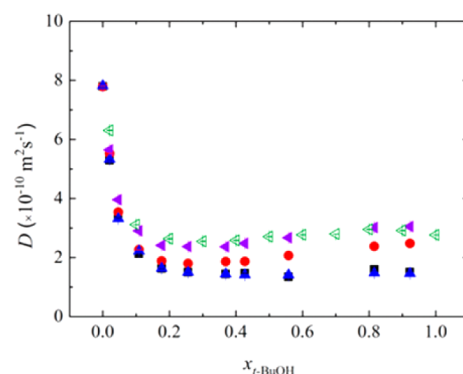


Figure 6. Diffusion coefficients (D) of R (■), C (red ●), and H (blue ▲) at ~ 15 mM and $t\text{-BuOH}$ (purple left-facing ▲) in samples at various $t\text{-BuOH}$ mole fractions ($x_{t\text{-BuOH}}$) in D_2O measured at 298 K. The data for $t\text{-BuOH}$ (green left-facing ▲) from the H_2O –alcohol system taken from ref 24 are shown for comparison.

The diffusion of $t\text{-BuOH}$ in this system followed the same trend as the H_2O – $t\text{-BuOH}$ system given in ref 24, which suggested that the water and $t\text{-BuOH}$ interact in a similar fashion in the two systems. For all $x_{t\text{-BuOH}}$ greater than zero, there was separation in diffusion of isomer C from the isomers R and H; in contrast, this separation only occurred in the case of EtOH for $x_{\text{EtOH}} > \sim 0.2$ (the separation is not fully evident in Figure 6 due to the size of the symbols). The separation gradually increased with higher $x_{t\text{-BuOH}}$. The diffusion of isomer C differed from R and H by over 30% at $x_{t\text{-BuOH}} \geq 0.55$, as compared to 18% for EtOH and 25% for 1-PrOH.

Ethylene Glycol. There was no separation of the diffusion coefficients for the R, C, and H isomers in the presence of ethylene glycol at the concentrations measured (Figure 7). Increasing ethylene glycol concentration resulted in a monotonic decrease of the isomer diffusion coefficients. This is in contrast to the diffusion behavior in the aqueous monohydric alcohol, which exhibited clear diffusive minima.

Stokes Radii. The Stokes radii of the R, C, and H isomers in D_2O –EtOH, D_2O –1-PrOH, D_2O – $t\text{-BuOH}$, and D_2O –ethylene glycol are shown in Figure 8a–d, respectively. The Stokes radii in Figure 8 were determined from eq 1 and the interpolated viscosity data; this interpolation calculated a lower viscosity at $x_{\text{A}} = 0$ than the known viscosity. Instead, using the known viscosity $\eta = 0.8903$ mPa s for $x_{\text{A}} = 0$ together with the measured diffusion data, the r_{S} values of the three isomers were

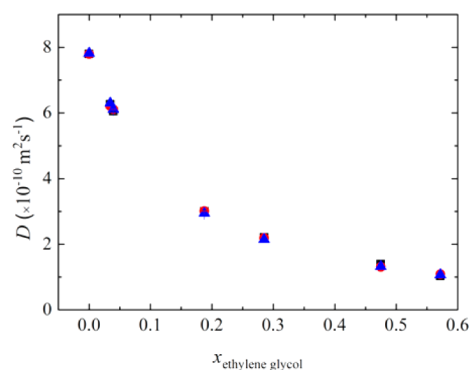


Figure 7. Diffusion coefficients (D) of R (■), C (red ●), and H (blue ▲) at ~ 15 mM at various ethylene glycol mole fractions ($x_{\text{ethylene glycol}}$) in D_2O measured at 298 K.

determined to be ~ 3.14 Å.⁶² This is larger than the van der Waals radii (r_W) of 2.86 Å calculated for the three isomers using values from the Edward and Bondi models.^{63–65} The effects of hydration are the likely reason for the difference between r_W and r_S . Taking the radius of water as 1.4 Å,^{66,67} the difference in volume between the measured r_S and r_W is approximately 2.75 water molecules. However, r_{S-C} becomes smaller than r_{W-C} when $x_A > 0.2$, which may be explained by the limitation of the Stokes–Einstein–Sutherland equation when the solute size is not much greater than the solvent. This makes direct comparison with r_W inapplicable; however, semiquantitative analysis was still possible by direct comparison of the measured r_S values for the isomers.

In the monohydric alcohol mixtures, considering $r_S = 3.14$ Å at $x_A = 0$, there was little change in r_S initially with increasing

x_A , and the isomers still had approximately the same r_S . The r_S values for each isomer increased in the regions $x_{\text{EtOH}} = 0.08–0.2$ and $x_{1-\text{PrOH}} = 0.05–0.1$, but not for $t\text{-BuOH}$. After the slight increase at $x_A < 0.1$, r_S decreased for all isomers with a greater decrease for r_{S-C} . For EtOH, the radii decreased slightly as x_{EtOH} approached 0.3–0.4 before r_{S-R} and r_{S-H} increased, whereas from $x_{\text{EtOH}} = 0.4$ r_{S-C} remained fairly constant (Figure 8a). For 1-PrOH, r_{S-C} continued to decrease, while r_{S-R} and r_{S-H} decreased slightly until $x_{1-\text{PrOH}} = \sim 0.3$, whereas r_{S-R} and r_{S-H} plateaued (Figure 8b). For $t\text{-BuOH}$, r_{S-C} continued to decrease, while r_{S-R} and r_{S-H} decreased slightly until $x_{t\text{-BuOH}} = \sim 0.38$, where they start to increase (Figure 8c). At higher concentrations, the larger r_S for the R and H isomers indicates that they may have a greater association with the solvent system. The greatest difference in r_S was seen in the $t\text{-BuOH}$ system.

The viscosity of water–ethylene glycol has a very different relationship with x_A than the water–monohydric alcohol systems. The viscosity increases almost linearly over the whole $x_{\text{ethylene glycol}}$ range, which corresponded with a slight increase in the isomer radii with increasing $x_{\text{ethylene glycol}}$. At higher $x_{\text{ethylene glycol}}$ the viscosity was greater than that of the monohydric alcohols.

Chemical Shift. A ^1H NMR spectrum of a mixture of the R, C, and H isomers in pure D_2O is given in Figure 9. The chemical shift (δ) of the resonances of each isomer changed with alcohol concentration (Figure 10), with each resonance experiencing a similar relative shift as x_{EtOH} , $x_{1-\text{PrOH}}$, or $x_{t\text{-BuOH}}$ increased. Initially, an increase in alcohol concentration caused an upfield shift (i.e., to lower ppm) until the concentration that corresponded with the lowest diffusion coefficients as shown in Figures 3, 5, and 6. Of note is that this region also

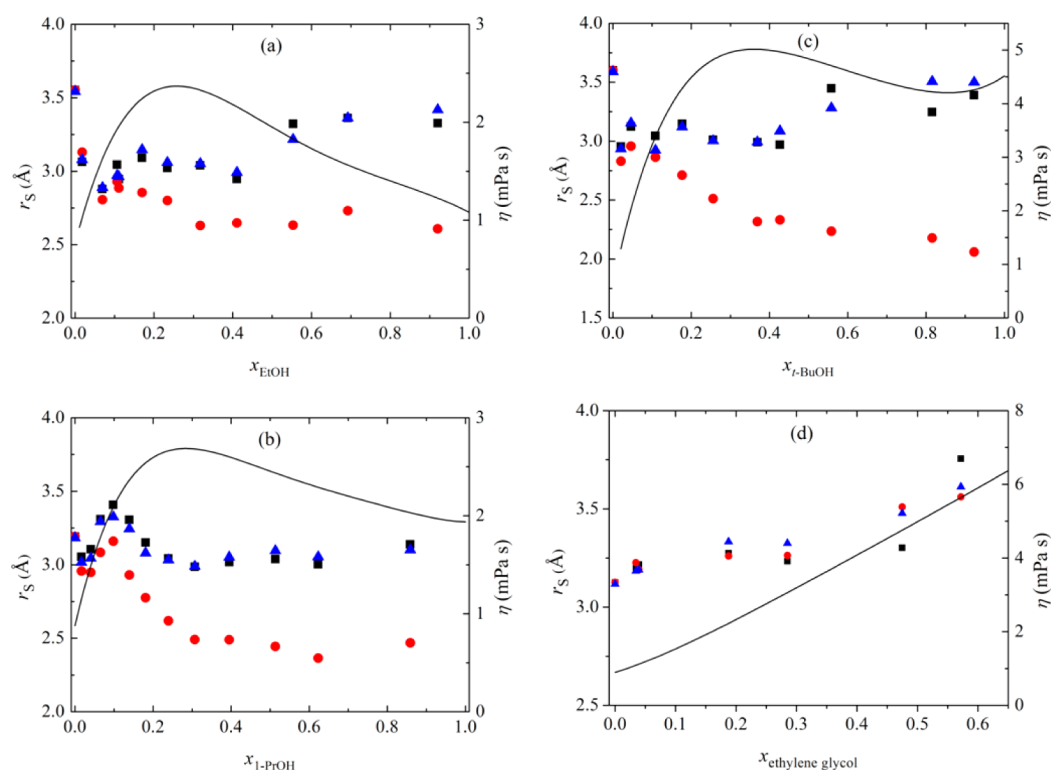


Figure 8. The Stokes radii (r_{S-R} (■), r_{S-C} (red ●), and r_{S-H} (blue ▲)) determined from the measured diffusion coefficient values and literature values of the solution viscosity for (a) water–EtOH,⁵⁶ (b) water–1-PrOH,⁵⁷ (c) water– $t\text{-BuOH}$,⁵⁸ and (d) water–ethylene glycol.⁵⁹ Viscosity values were determined by interpolation of literature values of viscosity data with a fifth-order polynomial (–).

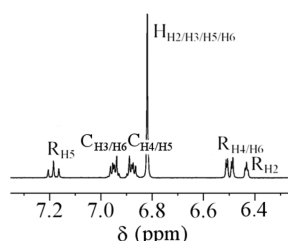


Figure 9. A ^1H NMR spectrum of the R, C, and H isomers in D_2O at 298 K. Subscripts denote the positions of hydrogen atoms shown in Figure 1. The symmetrically mirrored $\text{C}_{\text{H3/H6}}$ and $\text{C}_{\text{H4/H5}}$ resonances are an AA'XX' spin system.⁶⁸ Assignments were checked with MestReNova (Mestrelab Research S.L.).

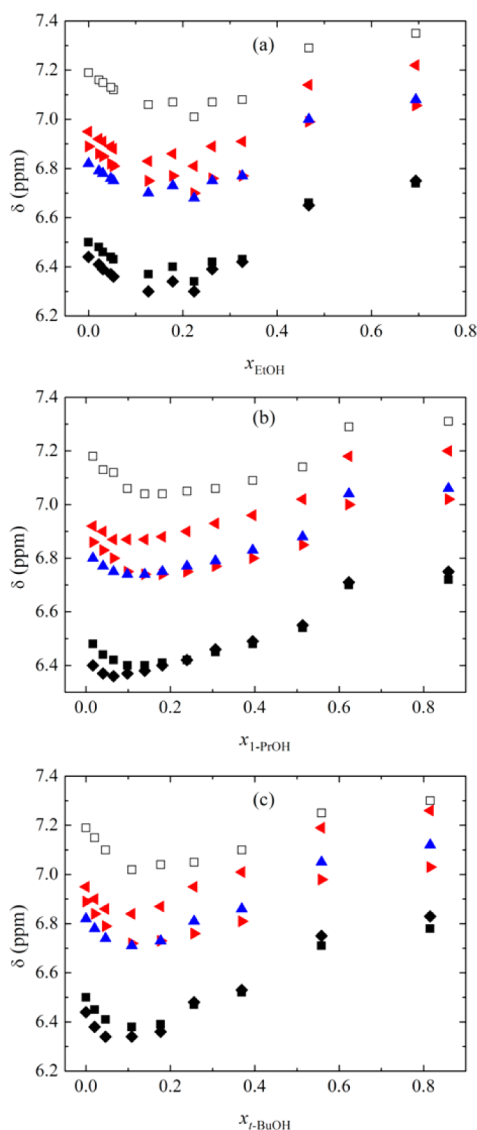


Figure 10. Change in chemical shift (δ) of the isomer resonances for R_{H5} (\square), $\text{R}_{\text{H4/H6}}$ (\blacksquare), R_{H2} (\blacklozenge), $\text{C}_{\text{H4/H5}}$ (red left-facing \blacktriangleleft), $\text{C}_{\text{H3/H6}}$ (red right-facing \blacktriangleright), and $\text{H}_{\text{H2/H3/H5/H6}}$ (blue \blacktriangle), at various x_{EtOH} (a), $x_{1\text{-PrOH}}$ (b), and $x_{t\text{-BuOH}}$ (c) in D_2O measured at 298 K. Refer to Figures 1 and 9 for the corresponding atom and resonance assignments.

corresponded with the greatest structuring of the solvents.²⁴ After this region, there is a downfield shift (i.e., to higher ppm) for all of the isomer resonances. There is also a change in the

chemical shift difference (ν_{AX}) between the $\text{C}_{\text{H3/H6}}$ and $\text{C}_{\text{H4/H5}}$ resonances (Figure 11a). The hydrogen atoms in C are in a

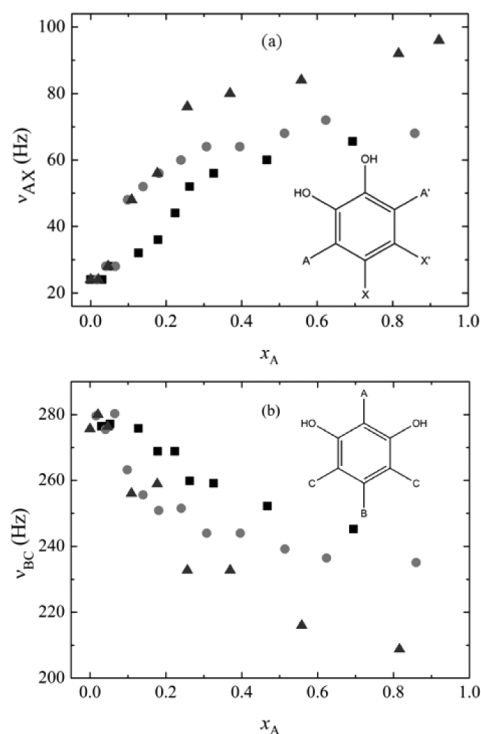


Figure 11. The chemical shift difference (ν) between the resonances for (a) $\text{C}_{\text{H3/H6}}$ (AA') and $\text{C}_{\text{H4/H5}}$ (XX') and (b) R_{H5} (B) and $\text{R}_{\text{H4/H6}}$ (C) protons is shown for various x_{EtOH} (\blacksquare), $x_{1\text{-PrOH}}$ (\bullet), and $x_{t\text{-BuOH}}$ (\blacktriangle) in D_2O measured at 298 K.

nonmagnetically equivalent AA'XX' spin system,⁶⁸ with the large split due to ν_{AX} between the A(A') and X(X') protons. Initially and at very low x_{A} , $\nu_{\text{AX}} = 24$ Hz. As x_{A} increased, ν_{AX} increased to >60 Hz for all monohydric alcohols. The increase in ν_{AX} corresponded with the separation of the C isomer from R and H isomers. There was also a difference in relative shift of the R resonances. The hydrogen atoms in R are in an ABC₂ spin system (Figure 11b). As x_{A} increases, the relative chemical shift difference ν_{BC} becomes smaller. The change in ν_{AX} and ν_{BC} increases with alcohol size (i.e., $t\text{-BuOH} > 1\text{-PrOH} > \text{EtOH}$). From Figure 10, it can be seen that the chemical shift difference between $\text{R}_{\text{H4/H6}}$ and R_{H2} initially starts with R_{H2} upfield at low x_{A} , but at high x_{A} , R_{H2} is downfield of $\text{R}_{\text{H4/H6}}$. This change is also greater with alcohol size (i.e., $t\text{-BuOH} > 1\text{-PrOH} > \text{EtOH}$).

DISCUSSION

Significantly different diffusion behavior of isomer C in comparison to isomers R and H was observed with increasing concentrations of EtOH, 1-PrOH, or $t\text{-BuOH}$ but not with ethylene glycol. Thus, it is pertinent to consider the solution structuring behavior of aqueous alcohol systems. A recent study, using Raman scattering to investigate the stretching bands of CH and OH groups in water–EtOH solutions, showed that the hydrogen bonds of EtOH hydrates, similar to a clathrate with 4.75 water molecules per EtOH, were strongest when $x_{\text{EtOH}} = 0.07\text{--}0.11$.²⁹ It was also concluded that there were structural rearrangements occurring in the $x_{\text{EtOH}} = 0.08\text{--}0.14$ range. Raman and IR spectroscopy was performed over the entire concentration range, $x_{\text{EtOH}} = 0\text{--}1$, to investigate

hydrogen bonding.²⁹ It was found that in the $x_{\text{EtOH}} = 0.06\text{--}0.09$ range the hydrogen bonding was at its strongest. A structural rearrangement in water–EtOH solutions was also proven, with clathrate-like structures in the $x_{\text{EtOH}} = 0.06\text{--}0.09$ range, which were then destroyed at higher concentrations. Neutron diffraction with isotope substitution was also used to investigate water–alcohol systems.^{30,31} In a $x_{\text{EtOH}} = 0.7$ mixture, it was found that water molecules existed in small hydrogen-bonded strings, with a preference for clusters of three water molecules,³¹ and isolated water molecules only made up $\sim 13\%$ of the sample. It was also shown that water had the net effect of causing the methyl head groups to be closer to each other. The formation of clusters in 1-PrOH–water, with up to 5 water molecules per propanol, was found using light scattering measurements.³² In the region, $x_{1\text{-PrOH}} = 0.15\text{--}0.2$, cluster formation was most significant. In the *t*-BuOH–water mixtures in the range $x_{t\text{-BuOH}} = 0.06\text{--}0.16$, it was found that the polar heads of *t*-BuOH preferred to bond with water through hydrogen bonding without alcohol–alcohol hydrogen bonding; however, the *t*-BuOH was still found in clusters due to hydrophobic interactions.³¹ These findings are in agreement with our results, and a detailed discussion is presented below.

At lower x_A where there was a dramatic decrease in the diffusion of both the monohydric alcohols and the isomers, the R, C, and H isomers could act similarly to the monohydric alcohols; that is, the isomer OH groups experienced hydrogen bonding primarily with the water molecules. In the regions of $x_{\text{EtOH}} = 0.2\text{--}0.3$, $x_{1\text{-PrOH}} = 0.1\text{--}0.2$, or $x_{t\text{-BuOH}} = \sim 0.2$, there were clathrate-like structures forming between the D₂O and alcohol molecules that slowed the diffusion of the isomers, which corresponded with the lowest *D* for the isomers. In these regions, the isomers could associate with water in a similar way as the alcohols and enter clathrate-like structures causing a lower *D*. This was based on the diffusion characteristics of the isomers being similar to that of the monohydric alcohols. Interestingly, in the EtOH system, once $x_{\text{EtOH}} > 0.2$ the diffusion of isomer C differed from isomers R and H. This is the same region where the solution dynamics of water and EtOH became increasingly independent.²⁴ Similar observations were made for the 1-PrOH and *t*-BuOH systems. In the regions $x_{\text{EtOH}} > 0.3$, $x_{1\text{-PrOH}} > 0.1$, and $x_{t\text{-BuOH}} > 0.2$, as the water and alcohol molecules became increasingly independent, the separation of C increased. This may be due to the fact that the weaker hydrophobicity of isomer C as compared to isomers R and H results in less interaction with the alcohol molecules at higher x_A .

That no separation of isomer diffusion coefficients was observed for the ethylene glycol system also suggests that hydrophobic interactions are involved in the monohydric alcohol cases. With its two hydroxyl groups, ethylene glycol forms hydrogen-bonded structures similar to water. This structuring may have prevented the isomers from diffusing differently, whereas in the case of monohydric alcohols, the greatest separation was at higher x_A when the solution structuring was at its least. This may have allowed the R and H isomers to form stronger hydrophobic interactions with the monohydric alcohols. Bayram et al.³⁷ found that the *ortho*-position of the OH groups on isomer C shielded the molecule from hydrophobic interactions, which may have been preventing the C isomer from having the same interactions with the monohydric alcohols as R and H.

That the R and H isomers had a greater interaction with the monohydric alcohols is supported by the Stokes radii data. The

r_s values of the R and H isomers were greater than those for C at higher x_{EtOH} , $x_{1\text{-PrOH}}$, and $x_{t\text{-BuOH}}$. From the present results, it appears that the R and H isomers had a greater association with the alcohol than the C isomer. The greatest difference in r_s occurred in *t*-BuOH, which has the largest hydrophobic region of the monohydric alcohols investigated. There was also an increase of the r_s values for each isomer below $x_A = 0.2$; this change corresponds with the solution structuring between water and the monohydric alcohols.

The chemical shift results indicate that all of the isomers experienced a changing environment across the x_A range. There was a distinct upfield shift in the region $x_A = 0.1\text{--}0.2$ corresponding to the greatest solution structuring as determined from the diffusion coefficients. The downfield shift at higher x_A and increases in diffusion coefficients suggest that there was further change in solution structuring, which was supported by the literature. The change in solution structuring at higher x_A , along with the greater concentration of monohydric alcohols, allowed the differential interaction between the monohydric alcohols and the R, C, and H isomers to become more apparent.

CONCLUSIONS

It was found that the diffusion of C differed from that of R and H in water–monohydric alcohol (EtOH, 1-PrOH, and *t*-BuOH) systems. It was proposed that the R and H isomers had a greater hydrophobic interaction with the monohydric alcohols as compared to the more polar C isomer. The degree of separation in diffusion increased at higher x_A corresponding to less solution structuring. The separation was greater in the *t*-BuOH–water system with *t*-BuOH having the largest hydrophobic region among the monohydric alcohols used in this study. One important potential use of a water–alcohol solution is to modify the diffusion behavior of molecules in a mixture and thus enable separation of the resonances of different species. The DOSY spectra in Figure 2 show the improvement of resolution in diffusion obtained just by changing the solvent mixture. A simple titration with, for example, ethanol can hence augment the power of DOSY and identify additional species in a matrix-assisted DOSY experiment.² The diffusion of these isomers is sensitive to changes in solution microstructure and therefore can be further used to probe solution dynamics. The results show that a clearer understanding of the solution dynamics of the water–alcohol systems can lead to improved matrix-assisted DOSY experiments.

ASSOCIATED CONTENT

Supporting Information

Schematic diagram for a stimulated spin–echo pulse sequence. This material is available free of charge via the Internet at <http://pubs.acs.org>.

AUTHOR INFORMATION

Corresponding Author

*Phone: +61 2 4620 3336. Fax: +61 2 4620 3025. E-mail: w.price@uws.edu.au.

Notes

The authors declare no competing financial interest.

ACKNOWLEDGMENTS

D.J.C. was supported by an Australian Postgraduate Award through the University of Western Sydney. The University of

Western Sydney is also acknowledged for financial support including a UWS IRIS grant. This work was also supported by the UK Engineering and Physical Sciences Research Council (Grant nos. EP/H024336/1 and EP/E05899X/1).

■ REFERENCES

- (1) Cohen, Y.; Avram, L.; Frish, L. *ChemInform* **2005**, 36, 520.
- (2) Evans, R.; Haiber, S.; Nilsson, M.; Morris, G. A. *Anal. Chem.* **2009**, 81, 4548.
- (3) Johnson, C. S., Jr. *Prog. Nucl. Magn. Reson. Spectrosc.* **1999**, 34, 203.
- (4) Price, W. S. *NMR Studies of Translational Motion*; Cambridge University Press: Cambridge; New York, 2009.
- (5) Stilbs, P. *Anal. Chem.* **1981**, 53, 2135.
- (6) Morris, K. F.; Johnson, C. S. *J. Am. Chem. Soc.* **1992**, 114, 3139.
- (7) Morris, G. A. *Diffusion-Ordered Spectroscopy. Encyclopedia of Magnetic Resonance*; John Wiley & Sons, Ltd.: New York, 2007.
- (8) Barjat, H.; Morris, G. A.; Smart, S.; Swanson, A. G.; Williams, S. C. R. *J. Magn. Reson.* **1995**, 108, 170.
- (9) Nilsson, M. *J. Magn. Reson.* **2009**, 200, 296.
- (10) Colbourne, A. A.; Morris, G. A.; Nilsson, M. *J. Am. Chem. Soc.* **2011**, 133, 7640.
- (11) Price, W. S.; Ide, H.; Arata, Y. *J. Phys. Chem. A* **1999**, 103, 448.
- (12) Price, W. S.; Ide, H.; Arata, Y. *J. Chem. Phys.* **2000**, 113, 3686.
- (13) Price, W. S.; Ide, H.; Arata, Y.; Söderman, O. *J. Phys. Chem. B* **2000**, 104, 5874.
- (14) Tormena, C. F.; Evans, R.; Haiber, S.; Nilsson, M.; Morris, G. A. *Magn. Reson. Chem.* **2010**, 48, 550.
- (15) Cassani, J.; Nilsson, M.; Morris, G. A. *J. Nat. Prod.* **2012**, 75, 131.
- (16) Tormena, C. F.; Evans, R.; Haiber, S.; Nilsson, M.; Morris, G. A. *Magn. Reson. Chem.* **2012**, 50, 458.
- (17) Adams, R. W.; Aguilar, J. A.; Cassani, J.; Morris, G. A.; Nilsson, M. *Org. Biomol. Chem.* **2011**, 9, 7062.
- (18) Rogerson, A. K.; Aguilar, J. A.; Nilsson, M.; Morris, G. A. *Chem. Commun.* **2011**, 47, 7063.
- (19) Penner, N. A.; Nesterenko, P. N. *Analyst* **2000**, 125, 1249.
- (20) Ray, S.; Takafuji, M.; Ihara, H. *J. Chromatogr., A* **2012**, 1266, 43.
- (21) Xu, D.; Dong, X.; Zhang, H.; Wang, H.; Jiang, P.; Zhang, M. *J. Sep. Sci.* **2012**, 35, 1573.
- (22) Yao, L.-F.; He, H.-B.; Feng, Y.-Q.; Da, S.-L. *Talanta* **2004**, 64, 244.
- (23) Shao, Q.; Fan, Y.; Yang, L.; Gao, Y. Q. *J. Chem. Phys.* **2012**, 136, 115101.
- (24) Price, W. S.; Ide, H.; Arata, Y. *J. Phys. Chem. A* **2003**, 107, 4784.
- (25) Yoshida, K.; Kitajo, A.; Yamaguchi, T. *J. Mol. Liq.* **2006**, 125, 158.
- (26) Corsaro, C.; Maisano, R.; Mallamace, D.; Dugo, G. *Physica A* **2013**, 392, 596–601.
- (27) Corsaro, C.; Spooren, J.; Branca, C.; Leone, N.; Broccio, M.; Kim, C.; Chen, S.-H.; Stanley, H. E.; Mallamace, F. *J. Phys. Chem. B* **2008**, 112, 10449–10454.
- (28) Burikov, S.; Dolenko, S.; Dolenko, T.; Patsaeva, S.; Yuzhakov, V. *Mol. Phys.* **2010**, 108, 739.
- (29) Burikov, S.; Dolenko, T.; Patsaeva, S.; Starokurov, Y.; Yuzhakov, V. *Mol. Phys.* **2010**, 108, 2427.
- (30) Finney, J. L.; Bowron, D. T.; Soper, A. K. *J. Phys.: Condens. Matter* **2000**, 12, A123.
- (31) Dixit, S.; Crain, J.; Poon, W. C. K.; Finney, J. L.; Soper, A. K. *Nature* **2002**, 416, 829.
- (32) Großmann, G. H.; Ebert, K. H. *Ber. Bunsen-Ges.* **1981**, 85, 1026.
- (33) Jeffrey, G. A. *An Introduction to Hydrogen Bonding*; Oxford University Press: New York; Oxford, 1997.
- (34) Saiz, L.; Padro, J. A.; Guardia, E. *J. Chem. Phys.* **2001**, 114, 3187.
- (35) Petterson, K. A.; Stein, R. S.; Drake, M. D.; Roberts, J. D. *Magn. Reson. Chem.* **2005**, 43, 225.
- (36) Vital de Oliveira, O.; Gomide Freitas, L. C. *J. Mol. Struct. (THEOCHEM)* **2005**, 728, 179.
- (37) Bayram, E.; Ayranci, E. *J. Chem. Thermodyn.* **2010**, 42, 1168.
- (38) Rudyk, R.; Molina, M. A. A.; Gómez, M. I.; Blanco, S. E.; Ferretti, F. H. *J. Mol. Struct. (THEOCHEM)* **2004**, 674, 7.
- (39) Rudyk, R.; Molina, M. A. A.; Gómez, M. I.; Blanco, S. E.; Ferretti, F. H. *Internet Electron. J. Mol. Des.* **2004**, 3, 11.
- (40) Kabanda, M. M.; Mammino, L. *Int. J. Quantum Chem.* **2011**, 112, 519.
- (41) Ludwig, R. *Angew. Chem., Int. Ed.* **2001**, 40, 1808.
- (42) Geiger, A.; Rahman, A.; Stillinger, F. H. *J. Chem. Phys.* **1979**, 70, 263.
- (43) Alavi, S.; Takeya, S.; Ohmura, R.; Woo, T. K.; Ripmeester, J. A. *J. Chem. Phys.* **2010**, 133, 074505.
- (44) Soper, A. K.; Benmore, C. J. *Phys. Rev. Lett.* **2008**, 101, 065502.
- (45) Harris, K. R.; Woolf, L. A. *J. Chem. Eng. Data* **2004**, 49, 1064.
- (46) Mills, R. *J. Phys. Chem.* **1973**, 77, 685.
- (47) Stokes, G. G. *Trans. Cambridge Philos. Soc.* **1856**, 9, 8.
- (48) Einstein, A. *Investigations on the Theory of the Brownian Movement*; Dover Publications: New York, 1956.
- (49) Sutherland, W. *Philos. Mag.* **1905**, 6, 781.
- (50) Koenig, S. H. *Biopolymers* **1975**, 14, 2421.
- (51) Pelta, M. D.; Morris, G. A.; Stchedroff, M. J.; Hammond, S. J. *J. Magn. Reson. Chem.* **2002**, 40, S147.
- (52) Botana, A.; Aguilar, J. A.; Nilsson, M.; Morris, G. A. *J. Magn. Reson.* **2011**, 208, 270.
- (53) Morris, G. A.; Barjat, H.; Home, T. J. *Prog. Nucl. Magn. Reson. Spectrosc.* **1997**, 31, 197.
- (54) Piotto, M.; Saudek, V.; Sklenář, V. *J. Biomol. NMR* **1992**, 2, 661.
- (55) Korson, L.; Drost-Hansen, W.; Millero, F. J. *J. Phys. Chem.* **1969**, 73, 34.
- (56) Kay, R. L.; Broadwater, T. L. *J. Solution Chem.* **1976**, 5, 57.
- (57) Mikhail, S. Z.; Kimel, W. R. *J. Chem. Eng. Data* **1963**, 8, 323.
- (58) Broadwater, T. L.; Kay, R. L. *J. Phys. Chem.* **1970**, 74, 3802.
- (59) Aminabhavi, T. M.; Gopalakrishna, B. *J. Chem. Eng. Data* **1995**, 40, 856.
- (60) Hawlicka, E.; Grabowski, R. *J. Phys. Chem.* **1992**, 96, 1554.
- (61) Pratt, K. C.; Wakeham, W. A. *Proc. R. Soc. London, Ser. A* **1975**, 342, 401.
- (62) Korosi, A.; Fabuss, B. M. *Anal. Chem.* **1968**, 40, 157.
- (63) Chan, T. C.; Chen, N.; Lu, J. G. *J. Phys. Chem. A* **1998**, 102, 9087.
- (64) Bondi, A. *J. Phys. Chem.* **1964**, 68, 441.
- (65) Edward, J. T. *J. Chem. Educ.* **1970**, 47, 261.
- (66) Gerstein, M.; Tsai, J.; Levitt, M. *J. Mol. Biol.* **1995**, 249, 955.
- (67) Zipper, P.; Durchschlag, H. *Physica A* **2002**, 304, 283.
- (68) Lambert, J. B. *Organic Structural Spectroscopy*; Prentice Hall: Upper Saddle River; London, 1998.